Plant Cell Reports (2022) 41:1209–1227
https://doi.org/10.1007/s00299-022-02850-5

ORIGINAL ARTICLE

Phylogeny and evolution of plant Phytochrome Interacting Factors (PIFs) gene family and functional analyses of *PIFs* in *Brachypodium distachyon*

Min Jiang[1,2] · Guosong Wen[3] · Changling Zhao[3]

Received: 21 December 2021 / Accepted: 14 February 2022 / Published online: 26 February 2022

Abstract

Key messages **Plant PIFs have been characterized, WGDs contributed to the expansion of class II PIFs; BdPIFs localized in the nucleus; BdPIF4/5C most likely response to high temperature and light stress.**

Abstract Phytochrome interacting factors (PIFs) belong to a small subset of basic helix-loop-helix (bHLH) transcription factors (TFs). As cellular signaling hubs, PIFs integrate multiple external and internal signals to orchestrate the regulation of the transcriptional network, thereby actuating the pleiotropic aspects of downstream morphogenesis. Nevertheless, the origin, phylogeny and function of plant PIFs are not well understood. To elucidate their evolution history and biological function, the comprehensive genomic analysis of the *PIF* genes was conducted using 40 land plant genomes plus additionally four alga lineages and also performed their gene organizations, sequence features and expression patterns in different subfamilies. In this study, phylogenetic analysis displayed that 246 *PIF* gene members retrieved from all embryophytes could be divided into three main clades, which were further felled into five distinct classes (Class I-V). The duplications of Class II PIFs were associated specially with whole genome duplication (WGD) events during the plant evolution process. Sequence analysis showed that PIF proteins had a conserved APB motif, and its crucial amino acid residues were relatively high proportion in the average abundance. As expected, subcellular localization analysis revealed that all BdPIF proteins were localized to the nucleus. Especially, BdPIF4/5C showed the highest expression level at high temperature, and the most significant hypocotyl elongation phenotype of overexpression of BdPIFs in Arabidopsis, which was consistent with the function and phenotype of AtPIF4. In brief, our findings provide a novel perspective on the origin and evolutionary history of plant PIFs, and lays a foundation for further investigation on its functions in plant growth and development.

Keywords bHLH · PIF · WGDs · *Brachypodium distachyon* · Functional evolution · Land plants

Abbreviations

PIF (PIL)	Phytochrome interacting factor-like
phys	Phytochromes
WGDs	Whole genome duplications
R	Red
FR	Far-red
bHLH	Basic helix-loop-helix
APB	Active phyB binding
APA	Active phyA binding
ROS	Reactive oxygen species

Communicated by Youn-Il Park.

✉ Min Jiang
20110700001@fudan.edu.cn

Guosong Wen
wengs@163.com

Changling Zhao
zhaoplumblossom7@163.com

[1] Ministry of Education Key Laboratory for Biodiversity Science and Ecological Engineering, Institute of Eco-Chongming (IEC), School of Life Sciences, Fudan University, Shanghai 200438, China

[2] Shanghai Key Laboratory of Plant Functional Genomics and Resources, Shanghai Chenshan Plant Science Research Center, Chinese Academy of Sciences (CAS), Shanghai Chenshan Botanical Garden, Shanghai 201602, China

[3] Research and Development Center for Heath Product, College of Agronomy and Biotechnology, Yunnan Agricultural University, Kunming 650201, Yunnan, China

FT	Flowing locus T
pI	Isoelectric point
Mw	Molecular weight
JTT	Jones-Taylor-Thornton
MEGA	Molecular evolution genetic analysis
ML	Maximum-likelihood
Clo-0	Columbia-0
MS	Murashige and Skoog
RT-qPCR	Real-time quantitative polymerase chain reaction
DAPI	4',6–Diamidino-2–phenylindole
RL	Rosette leaves
Days	Flowering time
SOD	Superoxide dismutase
POD	Peroxidase
CAT	Catalase
$\acute{\omega} = dN/dS$	Nonsynonymous-to-synonymous rates ratio
WGT	Whole-genome triplication
ORFs	Open reading frames
pifq	*pif1/3/4/5*

Introduction

Photoreceptor molecules in plants are responsible for light perception and the initiation of signal responses, which are crucial for survival and acquiring optimal status in a dynamically changing light environment. There are five phytochromes (phys) in Arabidopsis, namely phyA, phyB, phyC, phyD and phyE, which are responsible for perceiving and response to red (R) and far-red (FR) light spectrum (Clack et al. 1994; Legris et al. 2019). Phytochromes are converted between two interconvertible forms, when R absorbing, the inactive form Pr (R absorbing) located in the cytosol converted into active Pfr form the translocates into the nucleus (Klose et al. 2015). Photoactivated phyB regulates photomorphogenesis by integrating multiple signaling pathways by interacting with a set of basic helix-loop-helix (bHLH) transcription factors (TFs) known as PIFs (or PILs) (PHYTOCHROME INTERACTING FACTOR-LIKE) (Leivar and Quail. 2011). This kind of proteins belong to the group VII of bHLH superfamily with 15 members in *A. thaliana* (Heim et al. 2003). Thereinto, eight members are designated as PIF (PIF1-PIF8) in Arabidopsis, which all harbors a conserved APB (for active phyB binding) motif (also called PIL-motif) in N-terminal region (Khanna et al. 2004; Lee and Choi 2017). Moreover, PIF1 and PIF3 also contain additional APA (for active phyA binding) motif with a less conserved sequence, which is necessary for phyA binding (Al-Sady et al. 2006; Shen et al. 2008). Mutational analyses show that the four amino acids in the APB domain (ELxxxxGQ) provide the Pfr specificity for the physical interactions of phyB-PIF, and that the sequences on both sides of the amino acids may also affect the binding of phyB to a certain extent (Khanna et al. 2004). The C-terminus of PIF proteins bears the bHLH domain, which is responsible for the formation of homodimers or heterodimers with other bHLH proteins and DNA-binding with the protein (Bu et al. 2011; Hornitschek et al. 2009). In general, all PIFs can bind the G-box (5'-CACGTG-3') or PBE-box (5'-CACATG-3') of target gene promoter region to regulate target gene expression at the transcriptional level (Zhang et al. 2013).

PIFs are involved in maintaining the skotomorphogenic status of the etiolated seedlings and the repression of photomorphogenic development as negative regulators in darkness (Leivar and Monte 2014). However, they are promoted the photomorphogenic development through rapid phosphorylation, ubiquitination, and proteasome-mediated their degradation after the onset of light (Xu et al. 2015). The regulation of most light responses displays significant functional redundancy within the PIF family. For instance, AtPIF1, AtPIF3, AtPIF4, AtPIF5, and AtPIF7 inhibit phy-imposed seedling photomorphogenesis during deetiolation, under daytime growing conditions, and response to shading through varying degrees of overlapping redundancy (Leivar and Monte 2014). However, they also have distinct functions under certain environment. For example, AtPIF1 shows functional specificity in inhibiting light-dependent seed germination (Oh et al. 2004). Unlike other AtPIFs, AtPIF2 (also called PIL1) and AtPIF6 slightly positively regulates seedling deetiolation and seed dormancy in a certain light, respectively (Luo et al. 2014; Penfield et al. 2010). AtPIF1 and/or AtPIF3 regulate chlorophyll biosynthesis photosynthesis, and reactive oxygen species (ROS) responses by modulating the expression of a number of genes during deetiolation (Chen et al. 2013; Liu et al. 2013). In addition, AtPIF3 functions in hypocotyl growth by modulating the freezing tolerance (Xu and Deng. 2020) and stomatal opening (Wang et al. 2010a). Moreover, AtPIF4 and AtPIF5 directly interact with cryptochromes and bind to target gene promoters in response to blue light (Ma et al. 2016; Pedmale et al. 2016). AtPIF4 and AtPIF7 are essential for the early response to thermomorphogenesis and at least partially accompanied by the production of the growth promoting hormone auxin (Fiorucci et al. 2020; Koini et al. 2009). AtPIF4 also accelerates entering the reproductive stage of plants in a temperature-mediated manner by directly activating the expression of flowing locus T (FT) (Kumar et al. 2012). Interestingly, AtPIF8 inhibits phyA-induced FR light responses, rather than phyB-mediated (Oh et al. 2020).

Very little *PIFs* have been annotated in plants except for Arabidopsis, but at least the evidence of multiple *PIFs* have been found at genome-wide levels in other seed plants, including rice (Nakamura et al. 2007), tomato (Lee & Choi. 2017), *Malus domestica* (Zheng et al. 2020), and so on. Moreover, ZmPIF3.1 and ZmPIF3.2 have also been

characterized that interact with the Pfr form of ZmphyB1 and possess presumptive APA motifs (Kumar et al. 2016). Likewise, rice PIF protein OsPIF14 interacts with the Pfr form of OsphyB (Cordeiro et al. 2016). Moreover, non-vascular plants Marchantia MpPIF and Physcomitrium PpPILs contain APA motifs, but not APB motifs. Interestingly, MpPIF preferentially interacts with the MpPhy-Pfr through this conserved motif, indicating that PIFs interaction with phyB depending on APB motifs is a derived characterization of spermatophyte (Lee and Choi. 2017). However, the degradation mechanism of the liverwort PIFs is similar to that of Arabidopsis, suggesting that it seems to originate and evolve in the common ancestor of land plants. Therefore, the further tackling of PIFs evolutionary history can benefit to better understanding their function. What's more, the pattern of gene expansion is an important aspect of evolutionary history. Because gene duplication provides new opportunities and basic sources for evolutionary success, especially whole genome duplications (WGDs) (Van de Peer et al. 2009).

Brachypodium distachyon is a model plant for its small physical stature, self-pollinate, short life cycle, and a small diploid genome, to study relevant questions unique to the cereals and grasses (International Brachypodium. 2010). PIFs function as a hub that integrates hormonal and environmental signals to orchestrate regulation of the transcriptional network (Lau and Deng. 2010; Leivar and Quail. 2011). However, there is limited information on the origin and evolutionary history of them in entire plant species and their functional evolution in *B. distachyon*. Here, we investigated *PIF* genes using bioinformatics methods and analyzed their gene organization, conserved motifs, molecular evolution, gene duplication patterns and phylogenetic relationships throughout plant lineages. To better understand the function of *B. distachyon PIF* genes, expression patterns of these genes were surveyed under various tissues and stresses. Moreover, the subcellular localization analysis of BdPIFs was also performed and observed. Finally, heterogeneous overexpression of *BdPIFs* was performed in Arabidopsis displayed the phenotype of hypocotyl elongation in the light treatment condition and precocious flowering, especially the transgenic plants of BdPIF4/5C. In general, these results provided a new viewpoint on the origin and evolutionary history, and established a foundation for further functional research of plant PIFs.

Methods and materials

Identification of *PIF* family members in land plant species

Detailed information about the Arabidopsis *PIF* gene was obtained from The Arabidopsis Information Resources database (TAIR: http://www.arabidopsis.org/) (Lamesch et al. 2012). Putative *PIF* genes of other plant species were identified by BLASTP searches across the set of orthologous protein sequences of *A. thaliana* in the publicly available PLAZA database (http://bioinformatics.psb.ugent.be/plaza/) (Van Bel et al. 2018) and/or phytozome database (https://phytozome-next.jgi.doe.gov/) (Goodstein et al. 2012). When the protein harbored HLH domain (IPR011598) and APB motif used in this search, it was considered as a candidate protein and was scanned by InterPro software for final confirmation. In addition, all identified proteins were examined for redundancy, without considering any alternative splice variants.

Sequence alignment, protein motif, phylogenetic tree and molecular evolution analyses

Multiple sequence alignments were performed using the Clustal Omega (http://www.ebi.ac.uk/Tools/msa/clustalo/). The conserved residues and PIL motifs in the alignments were executed using InterProScan against protein database (http://www.ebi.ac.uk/interpro/). Visualization of alignment logos of the protein conserved domain were generated using WebLogo (http://weblogo.threeplusone.com/). The structure schematic of the PIFs was achieved based on the InterProScan results. The theoretical isoelectric point (pI) and molecular weight (Mw) of PIFs was predicted by the online Compute pI/Mw tool (http://web.expasy.org/compute_pi/). DNASP v5.10 was used to counting Ka and Ks values and their ratios of candidate PIFs aligned cDNA sequences (Librado & Rozas. 2009). The genetic distances of between each group were calculated with the Jones-Taylor-Thornton (JTT) model in the Molecular Evolution Genetic Analysis 6.0 (MEGA 6.0) (Tamura et al. 2013). MEGA6 software was also used to calculate the overall mean distances of all PIFs. The phylogenetic tree was reconstructed by IQTREE (Nguyen et al. 2015) using trimmed multiple alignments with the JTT + I + G model selected by ProtTest. A total of 1,000 bootstrap replicates were performed for support estimation.

Plant materials and growth conditions

B. distachyon and *A. thaliana* plants were grown in a soil mix (clay is mixed with soil at 3:1 ratio) and placed in a greenhouse with 22 ℃ and 70% room humidity under a 14-h-light (> 3000 lx) /10-h-dark photoperiod. *Nicothiana benthamiana* plants were grown in growth room conditions (16 h light at 26 °C and 8 h dark at 22 °C). All *A. thaliana* lines used in this study were in the Columbia-0 (Clo-0) background. Arabidopsis and *B. distachyon* seeds were surface-sterilized with 75% ethanol for 1 min, 10% bleaching powder for 10 min, then washed with sterilized water three times at least and sown on

sterile Murashige and Skoog (MS) medium containing 1.5% agar. Seeds were placed for 1 week at 4 °C in darkness and then transferred to a phytotron set at standard conditions or in continuous light (100 µmol m^{-2} s^{-1}) and constant temperature for specific experiments.

Expression analysis

The real-time quantitative polymerase chain reaction (RT-qPCR) was used to quantify the mRNA level of the *BdPIFs* genes, *Actin* as an internal control. For different tissue analysis, root, stem, leaf, caryopsis and seedling samples was harvested from 2-week-old *B. distachyon* Bd21 plants grown in 1/2 MS solid medium. For phytohormone analysis, 2-week-old seedlings were grown in 1/2 MS liquid medium containing 100 µM ABA for 1 h, 3 h, 6 h, 12 h and 24 h, respectively. For abiotic stress analysis, light treatment, UV-B and heat conditions were treated by placing 2-week-old seedlings in 1/2 MS liquid medium at shade, UV-B and 40 °C for 1 h, 3 h, 6 h, 12 h and 24 h, respectively. For biotic stress, the leaves of seedlings were exposed in spray inoculation with a suspension of *Magnaporthe grisea* (Guy11, avirulent ace1 genotype; PH14, virulent ace1 genotype) or *Fusarium graminearum* (F0968) conidia and sampled at 4 h and 12 h after treatment. Untreated plants were served as control samples. Seedlings were collected at different time points after treatment and immediately frozen with liquid nitrogen.

Total RNA was isolated using Trizol reagent and reverse-transcribed into cDNA using PrimeScript RT Master Mix Perfect Real Time (TaKaRa) according to the manufacturer's instructions. The integrity of total RNA was evaluated by electrophoresis, and optical density readings were quantified using Nanodrop1000. The RT-qPCR assay was implemented in a 10 µl reaction with 5–50 ng of first-stand cDNA products (4 µl), 5 pmol of each primer (0.4 µl), 5 µl SYBR green master mix (Takara Co., Ltd, China) and 0.2 µl ROX. To maximize the visibility of the bands, the number of PCR cycles for each gene was adjusted to 45. Three replicates were performed independently for each treatment, using three biological replicates. The relative expression of *BdPIF* genes was counted using $2^{-\Delta\Delta Ct}$ method. The up-regulated genes were defined as a fold-change greater than 2 with the p value of < 0.05 and a fold change of 0.5 or less was used to define down-regulated genes when the p value of < 0.05 with sample at 0 h as control. The primer-sets were listed in Table S1.

Plasmid construction, Arabidopsis transformation and subcellular localization assays

Full-length cDNAs encoding BdPIF4/5A was amplified from Bd21 plants using 12-p1300-F (KpnI) and 12-p1300-R (XbaI) primers (Table S2), and cloned into pCAMBIA1300 vector at KpnI/XbaI sites, yielding plasmid 35S:BdPIF4/5A which was used for *Agrobacterium*-mediated transformation of the Arabidopsis (Clough and Bent 1998). The transgenic plants were screened on 1/2 MS medium containing 25 µg/L hygromycin, and their mRNA levels were confirmed by RT-PCR. The acquisition for transgenic plants of other BdPIFs was executed in accordance with the above method.

For subcellular localization analysis, the coding sequence of BdPIF4/5A was also amplified with12-GFP-F (KpnI) and 12-GFP-R (XbaI) primers (Table S3), and cloned into modified pCAMBIA1300-GFP at KpnI/XbaI sites, yielding plasmid 35S:BdPIF4/5A-GFP, which was used for transient expression in *N. benthamiana* leaves. The agroinfiltrated leaves of *N. benthamiana* with 35S:BdPIF4/5A-GFP were cultured in a standard greenhouse and gathered at 48 h after *Agrobacterium* GV3101 infiltration. BdPIF4/5A-GFP fluorescence signals were excited by 488-nm ion argon laser and detected by Zeiss LSM 510 Meta confocal laser scanning microscope (Oberkochen, Germany) (Anderson et al. 2006). The subcellular localization analysis of other BdPIFs was also performed according to the above method.

Physiological and biochemical measurements

Measurements of hypocotyls length were recorded with IMAGE J software (http://www.rsb.info.nih.gov/ij). Flowering time was recorded by counting the number of rosette leaves and the number of days from the sowing day to the appearance of the first flower under long-day conditions (light/16 h: dark/8 h). The Arabidopsis seedlings treated by shading were used as samples for physiological and biochemical analysis. Simply, seedlings were grown in 1/2 MS solid medium under standard greenhouse for 8 days, then transferred to darkness condition (Other conditions being constant) for 2 days and collected for next analysis. Superoxide dismutase (SOD), peroxidase (POD) and catalase (CAT) activities were detected by spectrophotometry following previously described methods (Mittova et al. 2000; Wang et al. 2010b). A minimum of 20 independent seedlings were picked for hypocotyl measurement with Clo-0 as control. Each experiment was repeated with multiple biological times with similar results. For expression analysis of *SODs*, *PODs* and *CATs*, the seedlings of heterologous expression plants -were collected after 2 days under light treatments. The RT-qPCR analysis was performed according to the methods mentioned above.

Results

Identification and characterization of *PIF* genes in 40 land plant species based on the conserved PIL-motif

To explore the diversity and evolution of PIF proteins, identification of *PIF* gene family was performed from 40 publicly available genome of land plants that located at different evolutional positions (Fig. 1). The result showed that the numbers of PIFs varied from species to species across the entire land plant kingdom. However, canonical PIF were absent in several streptophyte algal lineages including *Micromonas commoda*, *Ostreococcus lucimarinus*, *Volvox carteri* and *Chlamydomonas reinhardtii* dwelling in seawater environments (Table S4). Finally, 246 non-redundant PIF sequences harboring the bHLH domain and PIL-motif were retrieved in total (Table S4). The diploid *Brassica oleracea* and *Glycine max* genome had the largest number of *PIF* genes, whereas the *Marchantia polymorph* contained one (Fig. 1). Moreover, *Brassica rapa* (13) and *Gossypium raimondii* (9) contained higher PIF numbers (Fig. 1, Table S4). It was worth noting that a novel member (OsPIF8) considered as PIFs in rice, which was slightly difference with previous research (Nakamura et al. 2007). Hence, the PIF members are all increased in corresponding monocotyledons, such as *Setaria italica* and *Zea mays* (Fig. 1, Table S4). In non-seed plants, only eight *PIF* genes were identified, including three in *Selaginella moellendorffii*, four in *Physcomitrium patens* and one in *M. polymorph*. In flowering plants, the expansion of *PIF* genes might be involved with the recursive polyploidy or ancient polyploidization events (Fig. 1). For example, the duplicated *G. max* genomes that retain evidence of two rounds of WGDs (Jiao et al. 2011) had 14 *PIF* genes. Similarly, Brassica genomes undergone a Brassiceae-lineage-specific whole-genome triplication (WGT) (Liu et al. 2014) which might be contribute to the increase of gene number reach to 14 (Fig. 1).

Phylogenetic and molecular evolution analyses of PIFs

To investigate the evolution history of plant PIF proteins, the phylogenetic reconstruction of all identified 246 protein sequences composed of the conserved domains (APB and bHLH) from 40 land plants were performed based on sequence alignments of amino acids using ML methods. The phylogenetic tree clarified the number of main PIF lineages and the relationships between these. In this tree, PIF sequences resolved three main clades: Clade A (including PIF1, PIF4 and PIF5), Clade B (PIF7 and PIF8), and Clade C (PIF2, PIF3 and PIF6) (Fig. 2a). Because they include bryophyte sequences, all of sequences can probably be traced back to the origin of the land plants. Specially, Clade C can further split into two classes: class I (PIF3) and class II (PIF2 and PIF6), other clades have only one (Fig. 2a). Class I homologues comprised gymnosperms and angiosperms, forming a relatively well-supported clade (Fig. 2a, Table S4). In addition, Class I homologue was absent in *Carica papaya* (Table S4). As with the Class I PIF, Class V PIF contained gene members in gymnosperms and angiosperms, suggesting that they independently descended from a common ancestor of spermophyte. In addition, the sequence of Class V PIF was also absent in *Hordeum vulgare*. Class II PIF had gene members only in rosids including Brassicales, Malvales, Myrtales and Malpighiales, while Class IV PIF existed in almost all eudicots (Table S4). Ancient PIF consisted of only moss and fern PIF and had eight members. We named them based on the ancient roles of PIF3 clade than other members (although they were not on the same evolutionary branch with the Class I PIF), such as MpPIF3. The protein size of ancient PIF ranged from 211 (VvPIF8) to 853 (AcPIF3B) amino acids. Furthermore, Class III PIF exists only in angiosperms, indicating that they originated in the common ancestor of flowering plants.

Although the main three lineages of A, B, and C PIF have an ancient origin, their respective content has been shaped by many lineage-specific duplication events. Early duplications occurred in clades B and C of Gymnosperms (seed plants) to found the PIF2/3/6, and PIF7/8 lineages (Fig. 2b). Indeed, our phylogenetic tree showed that the present-day classes took place after the divergence of Lycophytes. In particular, the PIF sequences from ANA grade species indicated that these subfamilies were established before the initial radiation of the angiosperms. For instance, the PIF7 and PIF8 subfamilies each include sequences from ANA grade and other angiosperms (Fig. 2b). Interestingly, the duplication pattern of the PIF family is very consistent with the WGD that occurs during the evolution of seed plants (Jiao et al. 2011). Further analysis displayed that the parallel duplications occurred in several different PIF subfamilies prior to the radiation of the extant angiosperms, allowing what is called the preangiosperm duplication to play an important role in establishing the diversity of angiosperm PIF genes (Fig. 2b).

The genetic distance between Class I and II PIFs was 0.534, which was not the lowest than other counterparts, despite being located in adjacent evolutionary branches (Table 1), which was consistent with their evolutionary grouping (Fig. 2A). While the highest genetic distance difference occurred between Class II and Class V PIFs, suggesting that the sequence similarity between them were the

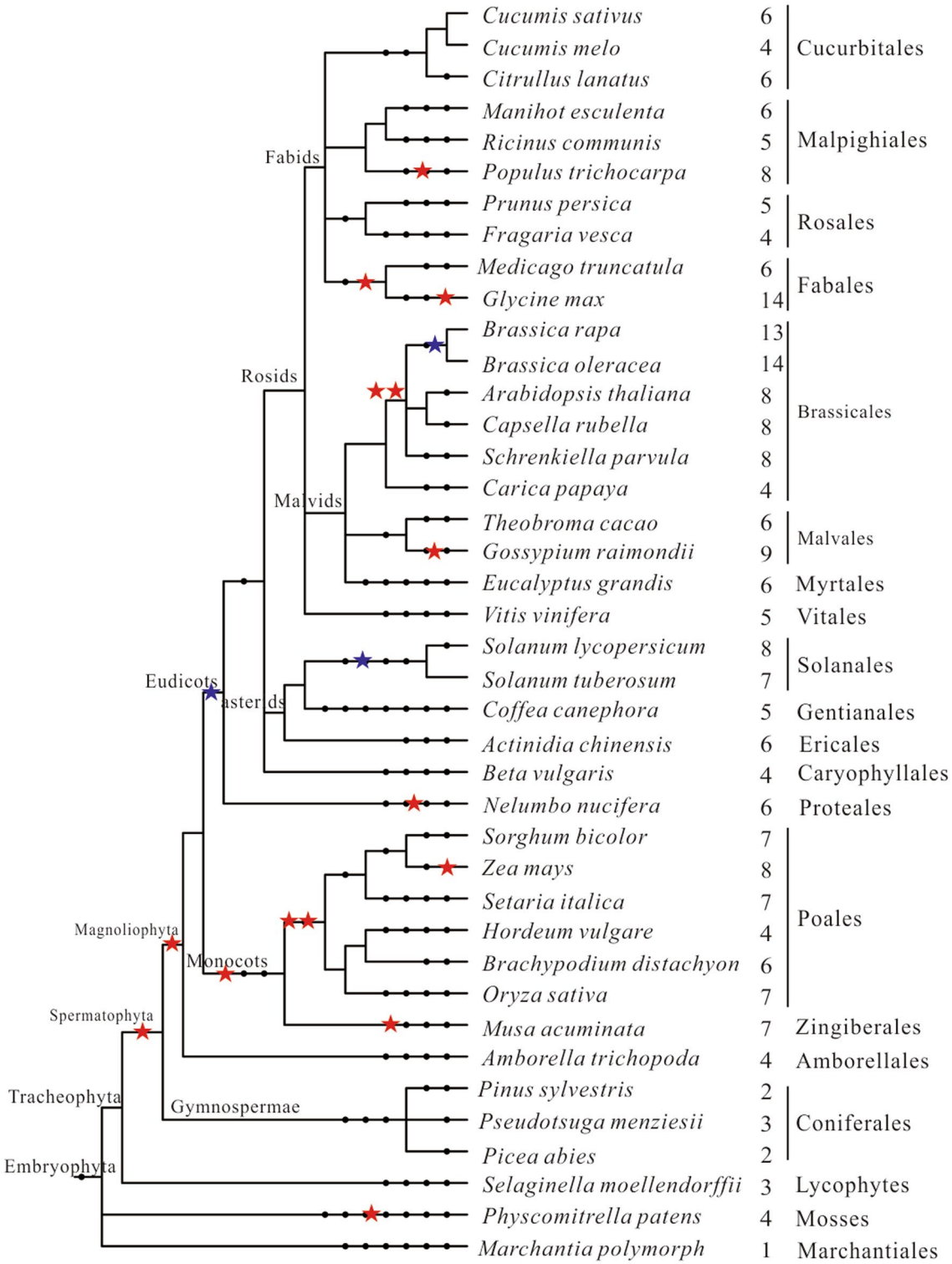

Fig. 1 Phylogenetic relationships between 40 plant species investigated in this study. The total number of PIF proteins identified in each plant genome is indicated on the right. The phylogenetic tree is modified from Phytozome (https://phytozome-next.jgi.doe.gov/). Red and blue stars indicate whole-genome duplication and triplication, respectively

least. In addition, the combination of Class V PIFs and other each group PIFs had relatively higher genetic distance than remaining counterparts (Table 1), indicating that Class V PIFs with other counterparts had higher sequence divergence. Interestingly, the average overall mean distance of PIFs was 0.452 (standard error 0.069). Moreover, the nonsynonymous-to-synonymous rates ratio ($\acute{\omega} = dN/dS$) of each group PIFs have been comprehensively calculated under different codon substitution-based evolutionary models to deeper analyze their evolutionary basis of functional diversification (Table 2). Molecular evolution analysis displayed that Class III PIFs had the lowest Ka and ώ values ($\acute{\omega} = 0.311$), reflecting strong purify selection during the evolution process (Table 2). While the mean ώ values of Class I, IV and V PIFs were greater than 1, suggesting that the *PIF* genes are positive selection during the evolution process. In addition, Class I and V PIFs had roughly similar Ka and ώ values when monocots were removed, which indicated that positive selection were mainly contributed to their evolution in Eudicots (Table 2). Moreover, we also surveyed the ώ values using the bHLH domain and APB motif sequences under different codon substitution-based evolutionary models. The results showed that all group PIFs had equally low Ka and ώ values, which were strong purify selection during the evolution process (Table S5). Molecular evolutionary analyses exhibited that the divergence of PIFs within each group were contributed to the sequences other than domain or motif, which indicated that their functional domains of PIFs were highly conserved.

Common conserved domain compositions and genomic analysis within plant PIF groups

To better understand the characteristics of different plant PIFs from an overview, the detailed sequence features were further surveyed. Not surprisingly, putative plant PIF proteins possessed common motifs in the same group, suggesting similar functions within each group. All of groups contained the bHLH domain (IPR011598) and the APB motif (Fig. 3a and b). It was noted that class I PIF (AtPIF3) and class IV PIF (AtPIF1) usually harbored APA motif (Fig. 3c). Moreover, a few PIF proteins also contained other domains, suggesting that PIF proteins might also have other functions. For instance, AtPIF7, BoPIF7, CruPIF7 and EgPIF1 extra contained a WD40/YVTN repeat-like-containing domain (IPR015943) (Fig. 3a). AcPIF1A and MaPIF8 also had a Zinc finger C2H2-type (IPR013087). An isopenicillin N synthase-like (IPR027443) and Remorin, C-terminal domains (IPR005516) also additional existed in NnPIF3B and FvPIF7, respectively. These data provided clues for us about other potential function of PIF proteins.

To elucidate the potential gene structural relationship among PIF orthologues and paralogues, their exon/intron organizations were also investigated using GSDS software. Most gene members within each group revealed similar exon/intron organizations in terms of intron number, intron phase and exon length. In particular, more similarities were observed in conserved regions such as bHLH domain (Fig. 3a). The numbers of intron varied from 0 to 10 among different members with wide variation (Table S6). Class II PIFs have introns ranged from 3 (*BoPIF6A*, *BoPIF6B*, and *BoPIF6C*) to 6 (*SpPIF6*) and 5 occupied the main points (58%), while the numbers of intron in Class V PIFs ranged from 0 (*CpPIF8*) to 9 (*MaPIF8*) and dominated with 5 (61%; Table S6). It was worth noting that most Class I, III and IV PIFs possessed 5 or 6 introns (Table S6).

Afterwards, the Mw and pI of different PIF proteins were also calculated using the online Compute pI/Mw tool. The Mw of PIF proteins ranged from 23.433 (VvPIF8) to 91.995 (MaPIF8) kDa and the pI varied from 4.82 (OsPIF4/5D) to 12.05 (SbPIF4/5C) (Table S6). It was interesting that the pI of all PIFs within each group ranged from acidic to alkaline. The average amino acid composition of PIF proteins were ranges from 0.71 (tryptophan) to 11.04 (serine) (Table S7). Notably, the average abundance of the most important amino acids such as glutamic acid, leucine and glycine (ELxxxxGQ) which is necessary and sufficient for phyB-specific binding were 5.38, 6.51 and 7.02, respectively. Moreover, the average abundance of their hydrophobic amino acids was relatively higher than ones of other amino acids such as alanine (8.28), leucine (6.51), proline (7.86) and valine (5.14) (Table S7).

Previous studies have reported several consensus sequences associated with the structural or functional roles, including the bHLH domain in C-terminal region, the APB motif and APA motif in N-terminal region. Most of all, the ELxxxxGQ in APB motif is required for phyB-specific binding (Khanna et al. 2004). To further identify the characteristic of consensus sequences among phylogenetic groups, the sequence logos motif analyses were then executed using WebLogo 3 online tool for each group to illustrate the sequences features of their key functional domain (Fig. 3b, c and Fig. S1). For example, the result displayed the detailed sequence information for APB or APA motif of each group (Fig. 3b and c). While the ancient PIFs may have difference (Inoue et al. 2016). The stars indicated that these residues were essential for the interaction PIFs with phytochrome. In all groups, the APB motif were highly conserved in spite of occasional variations such as EFPWEKDQ (AcPIF8) or EILWQNGQ (NnPIF4), indicating that most PIF had the function of binding to phyB (Fig. 3b). However, compared with APB motif, the APA motif was not highly conserved and existed only in Class I and IV PIF proteins (Fig. 3c). Furthermore, plant PIFs contained a highly conserved bHLH

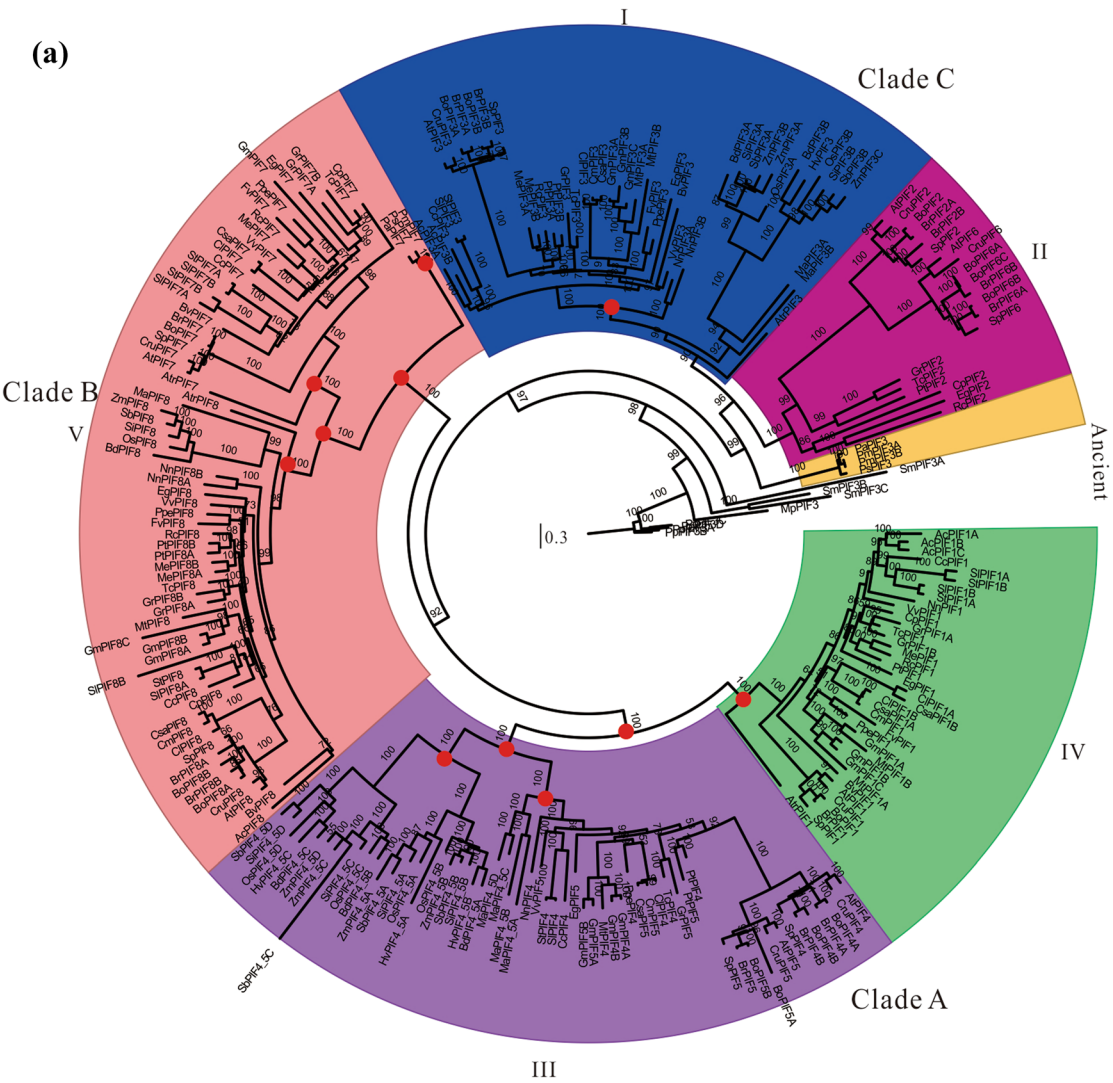
(a)
I
Clade C
II
Ancient
Clade B
V
IV
Clade A
III
0.3

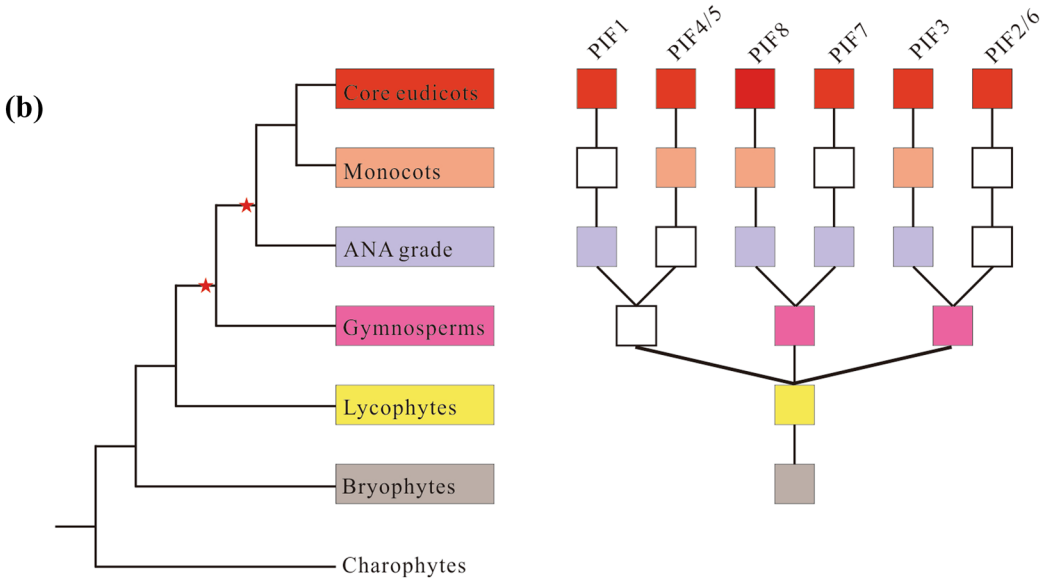
(b)
Core eudicots
Monocots
ANA grade
Gymnosperms
Lycophytes
Bryophytes
Charophytes
PIF1
PIF4/5
PIF8
PIF7
PIF3
PIF2/6

◂**Fig. 2** Phylogeny and expansion of PIF genes in land plants. **(a)** Phylogram of the 246-taxon analyses obtained through maximum-likelihood analyses were conducted using JTT + I + G. Support values are shown for selected nodes, bootstrap replicates BP. A dot indicates support values of BP > 95. Scale bar indicates number of changes per site. **(b)** Evolutionary origin of the PIFs. Filled squares indicate the presence of genomic data, open squares indicate lack of data, and red asterisks indicate a whole-genome duplication event (according to Jiao et al. 2011)

domain in C-terminal extension which comprised the HLH domain (dimerization) and basic domain (DNA binding capacity). The PIF proteins showed a group specific conserved basic domain except for Class II PIFs, H-N-X-S-E-R-R-R-R (Class I), H-N-L-S-E-R-R-R-R (Class III), H-N-L-S-E-R-R/K-R-R (Class IV) and H-N-Q/E-S-E-R-K/R-R-R (Class V), respectively (Fig. S1). The presence of group-specific basic domain in PIFs indicated that DNA binding capacity of PIFs might be have group specificity. Thus, it can be concluded that the evolution of different PIFs were orthologous based on group specificity.

Multiple duplication events were identified in each group

The main force in the evolution of different species is from gene duplication, which leads to the creation gene families from genes. To further comprehend the duplication and polyploidy or ancient polyploidization events of the *PIF* genes, the duplicated genes in land plant genome from each orthology group were also analyzed (Table S8). The number of duplicated genes was on behalf of the sizes of gene families which were usually called paralogous genes. As is well-known, plant species with duplicated genomes are more likely to cause gene duplications including *PIF* genes than those with unduplicated genomes. Thereby, *B. oleracea*, *B. rapa* and *G. max* had more duplicated genes. To further investigate the evolution and duplication events of each group of PIFs, their phylogenetic trees were reconstructed, respectively. The result showed that class I PIFs could be further divided into three subgroups according to the phylogenetic relationship of terrestrial plants, namely subgroup I1, I2, I3, I4 and I5 (Fig. S2). Of these five subgroups, subgroup I1, I2 and I3 contained genes in eudicots, whereas subgroup I4 contained genes from gymnosperms, and subgroup I5 only in monocots. Within the subgroup I3 clade, there were several independent duplications, suggesting that duplication events may have occurred in the ancestor of corresponding lineages (Fig. S2). Likewise, Class II and IV PIFs contained genes only in eudicots, whereas Class III and V PIFs contained genes from green plants and seed plants, respectively (Fig. S3-S6). Class III PIFs fell into seven subgroups, namely subgroup III 1–7 (Fig. S4). Of these subgroups, subgroup III 1–4 and III 5–7 contained genes in eudicots and monocots, respectively. While Class V PIFs were further divided into six subgroups, of which subgroup V1, V2, V4 and V5 contained genes from eudicots, while V3 and V6 only in monocots and gymnosperms, respectively (Fig. S6). Similarly, in the other clades, there were several independent duplications in Brassicales, Fabales and grasses (Figs. S4 and S6), which might be involved with two successive duplication events in Brassicales and at least three duplication events in grasses.

To further elucidate the causes of these duplication events occurred, we surveyed the genomic regions containing *PIF* genes that may be synteny. Most duplicate gene pairs emerged in syntenic genomic regions, implying that these multiple gene copies were resulted in whole genome or segmental duplications (Fig. 4). In particular, the duplication events of Class II PIFs, PIF2 and PIF6, have happed in the common ancestor of core eudicots which corresponded to the γ WGD (Fig. 4;(Tang et al. 2008)). The two duplications of Class II PIFs in Brassicaceae were associated with the α/β WGDs within the Brassicaceae lineage (Fig. S3; (Tang et al. 2008)). Based on extensive studies of WGD events in many species, these data about their paleopolyploidy histories were collected and deeper analyzed (Fig. 1). We then evaluated the impact of duplication events to the size of Class II PIFs. The result suggested that the WGDs might be beneficial to the orthology expansion of some species. For instance, compared with *Medicago truncatula*, *G. max* undergo one more genome polyploidization event, as a result, the soybean genome (14 *PIFs*) encoded more than two times numbers of family members (6 *PIFs*). To further confirm the roles of genome duplication in the expansion of gene family, the co-relationship analysis between rounds of genome duplication and encoded Class II PIFs were performed (Fig. S7). The correlation coefficient was counted as 0.939 ($P < 0.01$) for the Class II PIFs. The results indicated that the WGD prominently promoted to the gene expansion for Class II PIFs.

Expression profiles of the *PIF* genes in *B. distachyon*

Transcript profiling would offer direct clues of functional divergence among all members of a gene family (Whittle and Krochko 2009). In the study, RT-qPCR was performed to investigate the expression patterns of *BdPIF* genes in various tissues. The results showed that *BdPIF4/5A*, *BdPIF3B* and *BdPIF8* had expression in all tissues tested. *BdPIF4/5C* was highly expressed in root and the lowest in leaf, while *BdPIF4/5B* and *BdPIF3A* all had no expression in root (Fig. 5), suggesting that they may play distinct roles in the different tissues. To explore their roles in responses to hormone and abiotic stresses, the expression patterns of *BdPIFs* under ABA, light treatment, heat and UA-B conditions were also executed (Fig. 6). *BdPIF4/5A*,

Table 1 Genetic distance between different groups of *PIF* genes calculated based on the amino acid sequences with the Jones–Taylor–Thornton (JTT) model

	I	II	III	IV	V
I					
II	0.534				
III	0.314	0.664			
IV	0.229	0.576	0.268		
V	0.604	0.814	0.652	0.651	
Ancient	0.244	0.549	0.289	0.225	0.430

Table 2 Molecular evolutionary analysis of the *PIF* genes using their whole cDNA sequences

Group	N	Ka	Ks	ώ	G+C content
I	53	0.40124	0.30357	1.322	0.485
I*	39	0.35619	0.28795	1.237	0.444
II	20	0.37526	0.42332	0.886	0.430
III	58	0.22743	0.73132	0.311	0.526
III*	32	0.27979	0.61282	0.311	0.450
IV	37	0.30770	0.21808	1.414	0.508
V	65	0.31142	0.09072	3.433	0.518
V*	59	0.30764	0.09207	3.341	0.498
Ancient	8	0.44372	0.36284	1.223	0.513

N number of sequences, *Ka* the number of nonsynonymous substitutions per nonsynonymous site, *Ks* the number of synonymous substitutions per synonymous site, ώ, Ka/Ks. *Sequences from monocots were excluded

BdPIF4/5B and *BdPIF3A* showed increases after shading treatments and peaked at 3 h, then remained at relatively high levels. *BdPIF3B* exhibited increases and peaked at 12 h after treatment. *BdPIF4/5C* and *BdPIF8* were down-regulated at 1 h after treatment and kept at relatively low levels (Fig. 6a). Moreover, compared other *BdPIF* genes, *BdPIF4/5C* displayed the highest expression after heat treatment and peaked at 6 h, then remained at relatively high levels (Fig. 6b). However, all *BdPIF* genes except *BdPIF3B* were suppressed after UV-B treatment in spite of the times and extents of response had a difference (Fig. 6c). Furthermore, *BdPIF3A* and *BdPIF3B* were not induced by ABA within 1 h and then strongly suppressed at 3 h after treatment, while other *BdPIF* genes were strongly inhibited within 1 h (Fig. 6d). We also investigated their expression profiles after phytopathogen applications. *BdPIF4/5C*, *BdPIF3A* and *BdPIF8* were all significantly down-regulated after Guy11, PH14 and F0968 infection, while *BdPIF3B* only suppressed by Guy11 at 4 h and then recovered to near normal levels (Fig. 6e). In addition, *BdPIF4/5A* and *BdPIF4/5B* all revealed a slightly suppressed expression after inoculated pathogen (Fig. 6e).

BdPIF genes are nucleus localized TFs

To study the subcellular localization of BdPIFs, the six *BdPIF* open reading frames (ORFs) were cloned in pCAMBIA1300-GFP modified vector, respectively, followed by recombination and in-frame fusion to with GFP at C-terminal and expressed transiently in leaves of *N. benthamiana* plants and fluorescent signals were observed at 48 hpi (hours post-incubation), by confocal microscopy. Microscopic observations of the *N. benthamiana* leaves displayed that all BdPIFs-GFP fusion were distributed in the nucleus, being uniformly distributed in this compartmental localization, while GFP alone was localized in ubiquitously throughout the cell without specific compartment (Fig. 7). These results suggested that all *BdPIF* genes were nucleus-localized TFs, like the localization of Arabidopsis AtPIFs and maize ZmPIFs (Al-Sady et al. 2006; Wu et al. 2019).

Heterologous expression of *BdPIF* genes in Arabidopsis plants

To better characterize the physiological functions of *BdPIF* genes, the genetic studies in *B. distachyon* with reference to the light responses of plants were performed. The Arabidopsis plants (ecotype Col-0) were successfully transformed with *35S::BdPIF4/5A*, *35S::BdPIF4/5B*, *35S::BdPIF4/5C*, *35S::BdPIF3A*, *35S::BdPIF3B* and *35S::BdPIF8*. The RT-PCR results displayed that all the genes were overexpressed in corresponding transgenic lines (Fig. S8). The transgenic lines obtained were designated *BdPIF4/5A-OX* (over-expressor), *BdPIF4/5B-OX* and so on. To accurately assess the results, an Arabidopsis transgenic line *35S::AtPIF4* which showed the long-hypocotyl phenotype (Sun et al. 2012) was employed as positive control. As expected, the various *BdPIF-OX* transgenic plants showed similar hypocotyls elongation phenotype, especially *BdPIF4/5C-OX*, although the extents of hypocotyls elongation ranged obviously from one *BdPIF-OX* to another (Fig. 8a and b). In addition, we also investigated numbers of rosette leaves (RL) and flowering time (Days) of *BdPIF4/5C-OX*. It was found that three *BdPIF4/5C-OX* lines showed little numbers of rosette leaves and early flowering phenotype, as similar with phenotype of *AtPIF4-OX* plants (Fig. S9).

Moreover, the activities of SOD, POD and CAT of various *BdPIF-OX* transgenic plants were also performed. The activities of SOD of all *BdPIF-OX* transgenic plants were lower than that in Col-0 under light treatment condition, which was opposite in *AtPIF4-OX*, while they had no obvious difference under normal condition except *BdPIF4/5B-OX* and *BdPIF8-OX* (Fig. 8c). The activities of POD and CAT of Col-0, *AtPIF4-OX* and *BdPIFs-OX* samples all had no apparent change (Fig. 8d and e). Furthermore, we next surveyed the expression of *SOD*, *POD* and *CAT* genes in

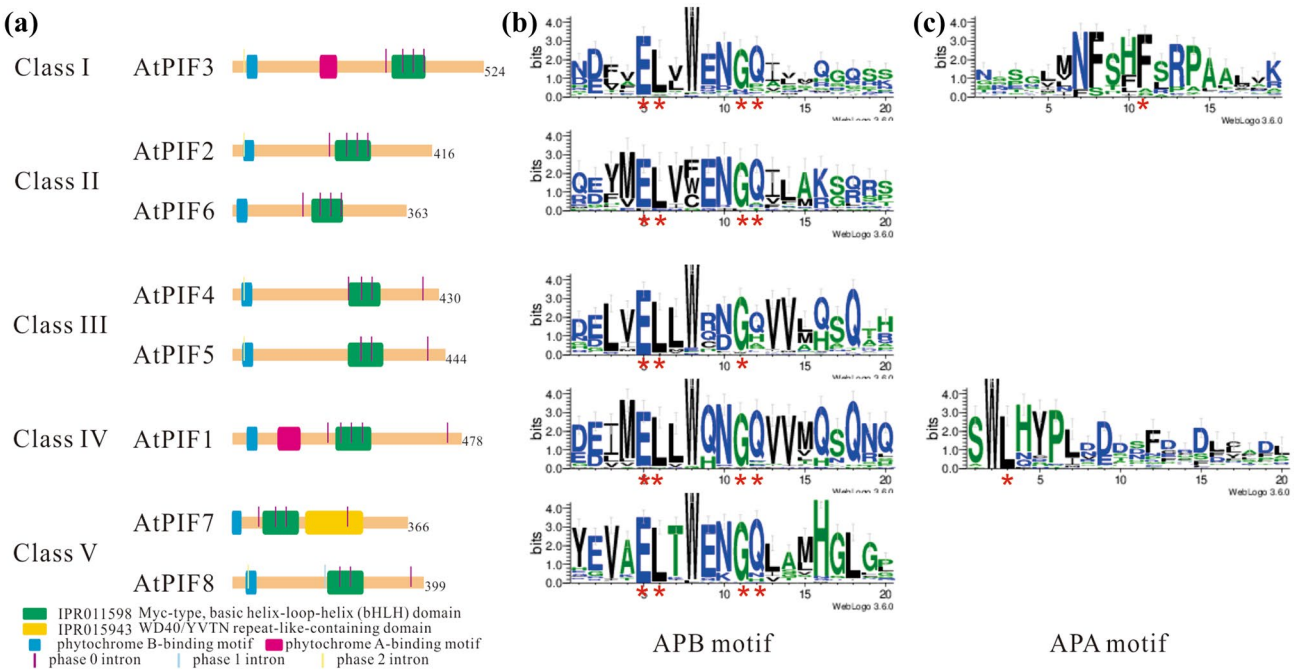

Fig. 3 Gene structure and sequence features of conserved *PIF* genes. **(a)** Gene structure and protein motif. The structure of an *A. thaliana* gene (indicated on the left) is shown as an example for each class (in parenthesis on the protein motifs are shown as colored boxes, whereas introns of different phase are shown as colored vertical lines. Protein motif architectures of the full-length proteins were drawn based on a search of interPro program. IPR011598 indicates basic helix-loop-helix (bHLH) domain, IPR015943 means WD40/YVTN repeat-like-containing domain. Exons are drawn to scale. **(b)** Sequence feature of APB domain. Sequence features shown in the form of web logos representing the conserved APB motif of each class. **(c)** Sequence feature of APA domain. The red star indicates residues of functional or structural importance based on phylogenetic conservations. Logos were generated using the Weblogo3 application (http://weblogo.threeplusone.com/)

various *BdPIF-OX* transgenic plants. A total of nine genes were screened for the present research including three *SOD* genes (*At5g18100*, *At2g28190* and *At3g10920*), three *POD* genes (*At5g66390*, *At5g58400* and *At2g18140*) and three *CAT* genes (*At4g35090*, *At1g20620* and *At1g20630*), which have been verified previously to be related to SOD, POD or CAT activity. The transcripts of almost all SODs, PODs and CATs displayed an increased significantly levels in *BdPIF-OX* transgenic plants under normal condition (Fig. S10). However, in various *BdPIF-OX* transgenic plants, the expression levels of all SODs, PODs and CATs showed different responses under light treatment condition, even significantly increased or decreased (Fig. S10). Moreover, SOD activities of different plants and under different conditions were the most significant difference. Therefore, we further analyzed the relationship between *SOD* gene expression results and actual activities. To evaluate their relationship between *SOD* gene expression results and actual activities, their correlation analysis was performed (Fig. S11). The correlation coefficient of *At5g18100* and *At2g28190* achieved a significant difference (Fig. S11). They are positively and negatively correlated under normal and light treatment conditions, respectively. These results indicated that these *SODs*, *PODs* and *CATs* genes were induced by BdPIFs to influence on the SOD, POD and CAT activity under normal condition, especially SOD activity. Taken together, these results suggested that the identified *BdPIF* genes were counterparts of Arabidopsis PIFs and exhibited a similar biochemical function to the AtPIFs.

Discussion

Evolutionary history and functional evolution of the *PIF* genes in land plant lineages

Our data suggested that the *PIF* gene family exist only in land plant lineages and is not even present in *M. viride* dwelling in subaerial/terrestrial (Fig. 1, Table S4). The *PIF* gene has expanded and subjected to at least two ancient duplications during the history of land plants. Following the gene duplication, the first expansion occurred after the divergence of Gymnosperms, leading to the emergence of the Clade C (Class I and class II) and other Clades, as consistent with their sequence divergence (Fig. 2a), resulting that Class I and II PIF members may experience a

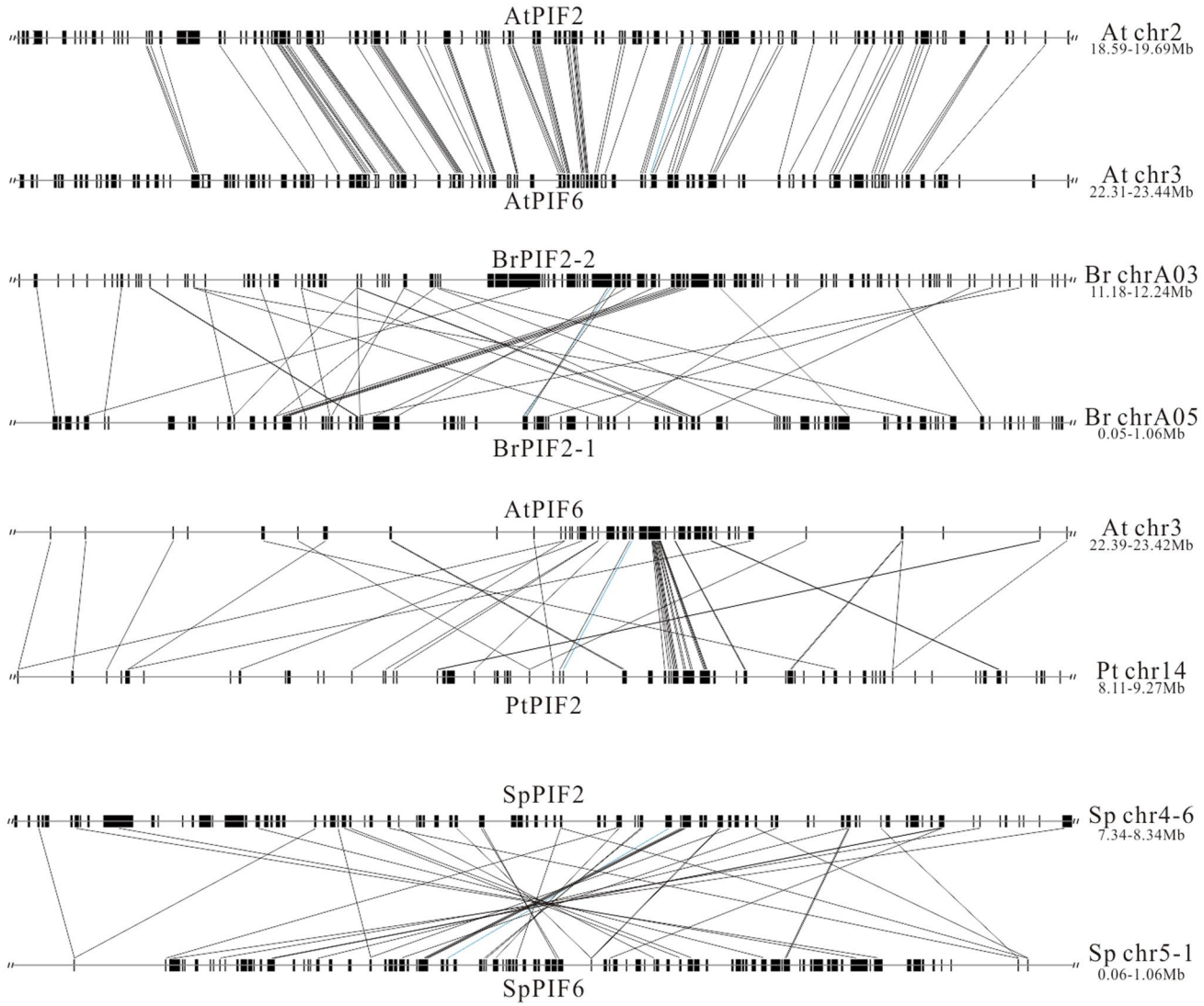

Fig. 4 Examples of the detailed locations of representative pairs of genes duplicated in recent polyploidy events in the syntenic regions. At, *Arabidopsis thaliana*; Br, *Brassica rapa*; Pt, *Populus trichocarpa*; Sp, *Schrenkiella parvula*; chr, chromosome

certain functional divergence. For instance, unlike most PIFs suppression of the light response, PIF2 and PIF6 shows a mild activation response under certain conditions (Luo et al. 2014; Penfield et al. 2010). In turn, the second expansion appeared after the divergence of angiosperms, resulting in two main Clades including Clade A (class III and IV) and Clade B (Class V) (Fig. 2) revealing apparent functional redundancy. For example, plants exhibited constitutive photomorphogenic phenotypes only in quadruple mutant (*pifq*, i.e. PIF1, PIF3, PIF4, and PIF5) in the dark (Leivar et al. 2008b; Shin et al. 2009). In addition, most PIFs inhibited light response and rapidly degraded upon light exposure, while PIF7 was not detected light-induced phosphorylation or degradation (Leivar et al. 2008a). The protein accumulation pattern and function of PIF8 were different from other PIFs under diverse light conditions (Oh et al. 2020). Further studies displayed that all plant PIFs shared highly similar exon/intron organizations with conserved APB motif and bHLH domains within each group (Fig. 3), indicating that these genes of ancient origins still maintained a fairly conservative role. However, expression profiles showed that all *BdPIF* genes were distinct expressed in different tissues (Fig. 5), indicating that it might be resulted in the evolutionary variation. Taken together, *PIF* gene members exhibit overlapping and distinct roles in different light responses, similar to the patterns of *HD-ZIP III* genes (Prigge et al. 2005).

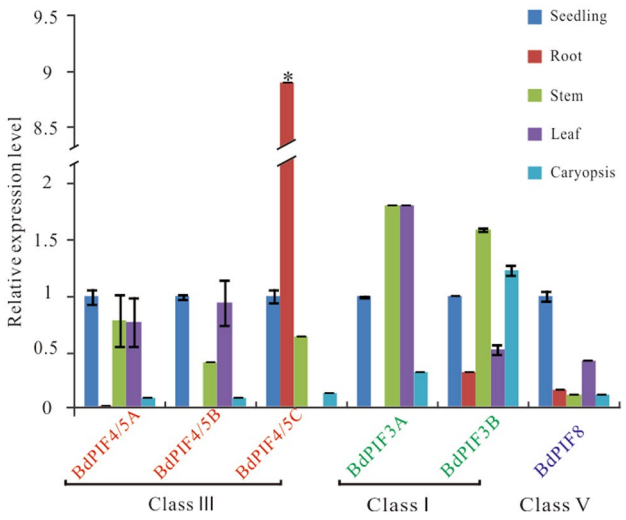

Fig. 5 Expression patterns of *BdPIF* genes in different tissues. Leaf, stem, seedling and root samples were collected 12 d after germination. Caryopsis samples were collected at their anthesis. The expression levels were normalized to the expression level of seedling. Stars indicate significant difference compared to seedling ($P < 0.05$). Bars represent SE ($n = 3$)

Whole genome duplication contributed to gene expansion of Class II PIFs

Our phylogeny suggested that there were two and/or three paralogs in the orthology groups of Class II PIFs. Further examination displayed that the genomic regions where the *PIF* genes were within syntenic genomic regions, implying that these multiple copies may be caused by large-scale duplication events such as WGDs or segmental duplications (Fig. 4). In particular, the duplication events of Class II PIFs took place in the common ancestor of core eudicots, corresponding to the γ WGD (Tang et al. 2008). Compared with *A. thaliana*, Brassica plants have undergone an extra recent whole-genome triplication (WGT) event (Jiao et al. 2012) resulted in the approximately twice as Class II PIF genes in *B. rapa* and *B. oleracea* than those of other species (Fig. 1 and Table S4), as in accordance with the discovery in other polyploids, including *Arachis hypogaea* (Wang et al. 2021) and *G. max* (Arya et al. 2018). Moreover, the correlation coefficient between the rounds of genome duplication and gene family size was 0.939 (Fig. S7), indicating a positive correlation of them. It have reported that the signaling genes and regulatory genes are more likely to be retained, mainly depending on their environmental adaptation after duplication events, rather than WGDs (Lei et al. 2012; Maere et al. 2005; Van de Peer et al. 2009). Although other forms of duplication also contribute to gene expansion, such as tandem duplication (Jiang et al. 2021), these independent and alike examples elucidated the function of WGDs in the gene expansion of Class II *PIF* genes, which existed in similar situations in other gene family such as *MKK* and/or *rhomboid* (Jiang & Chu. 2018; Li et al. 2015). The fact suggested that the WGDs and polyploidization events were helpful of the gene expansion of Class II *PIF* genes during their evolution process.

PIFs function as a cellular signaling hub in integrating environmental and hormonal pathways to modulate plant growth and development

Apart from being negative regulators of photomorphogensis, PIFs are also other crucial regulator that integrates various environmental and hormonal signaling for plant growth and development including temperature (Kumar et al. 2012; Xu and Deng. 2020), anthocyanin synthesis and accumulation (Liu et al. 2021; Shin et al. 2007), sugar metabolism (Liu et al. 2011), signaling pathways of plant hormones (GA, BR, NO, JA, Ethylene and auxin) (Leivar and Monte. 2014), and so on. In our study, expression analysis revealed that *BdPIF* genes could be induced by a variety of abiotic stresses and hormone (Fig. 6). Specially, six *BdPIF* genes were induced by shading and ABA treatments to produce variant response patterns, while *BdPIF4/5C*, compared with other *BdPIF* genes, was significantly up-regulated under heat stress (Fig. 6), as supported by previous studies (Choi and Oh. 2016; Koini et al. 2009). All *BdPIF* genes were inhibited after phytopathogen infection regarding of a difference in terms of time and extent (Fig. 6). The data suggested that the function of *BdPIFs* may be relatively conserved in response to external and hormonal signaling.

A growing body of evidence indicates that the identified *BdPIF* genes are orthologs of *AtPIFs*, as estimated from a biological perspective (Fig. 8). When the *BdPIF* TFs are expressed ectopically in Arabidopsis, the phenotype results of the transgenic plants were very similar to the morphology of AtPIF4 over-expressor, especially under light treatment condition, as in accordance with the elongated phenotype of *phyB* mutant (Leivar et al. 2012). Additionally, the

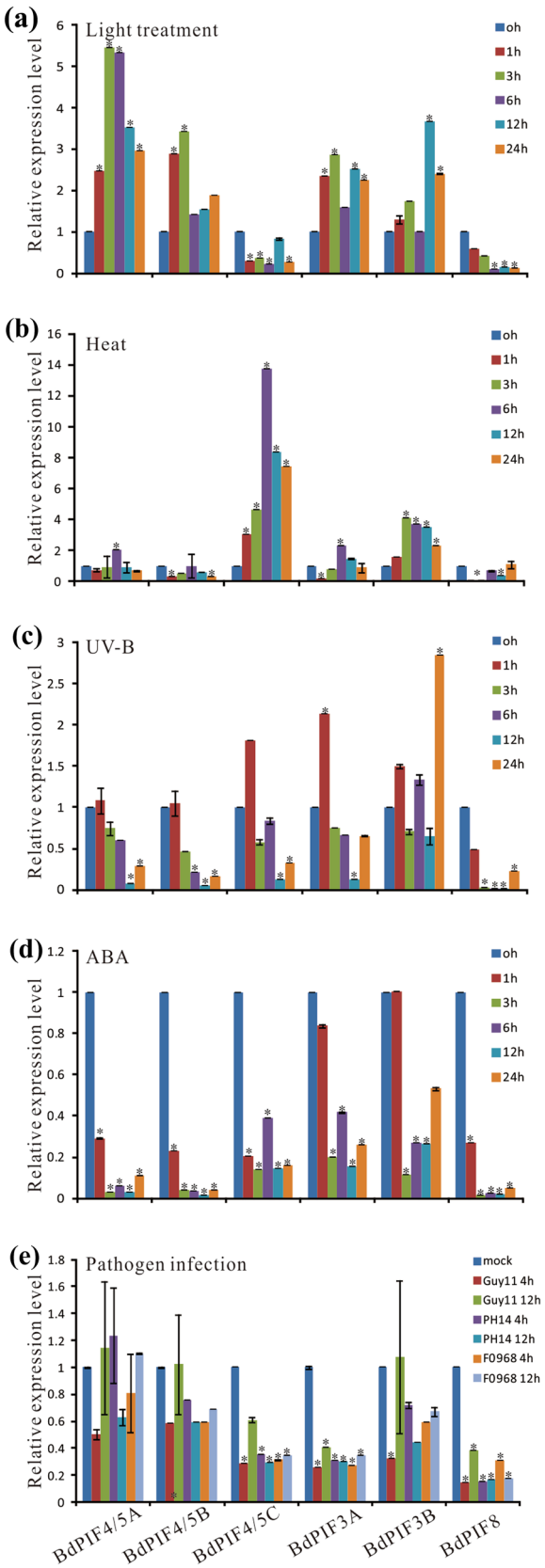

Fig. 6 Expression profiles of *BdPIF* genes under various stress treatments **(a)** Light treatment, **(b)** Heat, **(c)** UV-B, **(d)** ABA and **(e)** Pathogen infection. The expression levels were normalized by the *actin* gene. Stars indicate significant difference compared to seedling ($P < 0.05$). Bars represent SE (**n** = 3)

nuclear-localization and conserved APB motif of BdPIFs imply that it may play possible roles in plant growth and development (Figs. 3 and 7). Additionally, DELLA directly interacts with PIF and mediates its degradation in Arabidopsis (Li et al. 2016), while BdPIF3/4 also interacts with BdDELLA proteins (Niu et al. 2019), suggesting that genes from these two different species may have similar functions in both light and gibberellin signaling pathways. Notably, the *BdPIF4/5C* over-expressor displayed the most pronounced phenotype of hypocotyl elongated, precocious flowering and rosette leaves reduction, as is consistent with those of AtPIF4 over-expressor (Fig. S8) (Kumar et al. 2012). In addition, the expression of *BdPIF4/5C* and other *PIF* genes were significantly different under heat stress (Fig. 6). Therefore, our data suggest that *BdPIF4/5C* may play a vital role in plant adaptation to environmental and hormonal signaling, especially high-temperature, similar to AtPIF4.

Conclusion

A total of 246 *PIF* genes were identified by bioinformatics methods from 40 land plants based on the conserved bHLH domain plus the existence of APB motif, additionally algae lineages dwelling in subaerial/terrestrial were also analyzed. Phylogenetic analyses showed that the *PIF* gene family fell into five classes and designated as Class I to Class V. It was noteworthy that the expansion of Class II PIFs benefited by the WGDs followed by diversification during the evolution process. Moreover, molecular evolutionary and protein domain analyses revealed that the functional domains of PIFs were highly evolutionary conserved, especially the APB motif. Furthermore, all *BdPIF* genes were nucleus-localized TFs like the localization of Arabidopsis AtPIFs. Interestingly, it was found that *BdPIF4/5C* had the highest expression level after heat treatment and his over-expressor had the most conspicuous hypocotyls elongation and precocious flowering phenotype, which was in accordance with the function and phenotype of *AtPIF4*. In short, these results

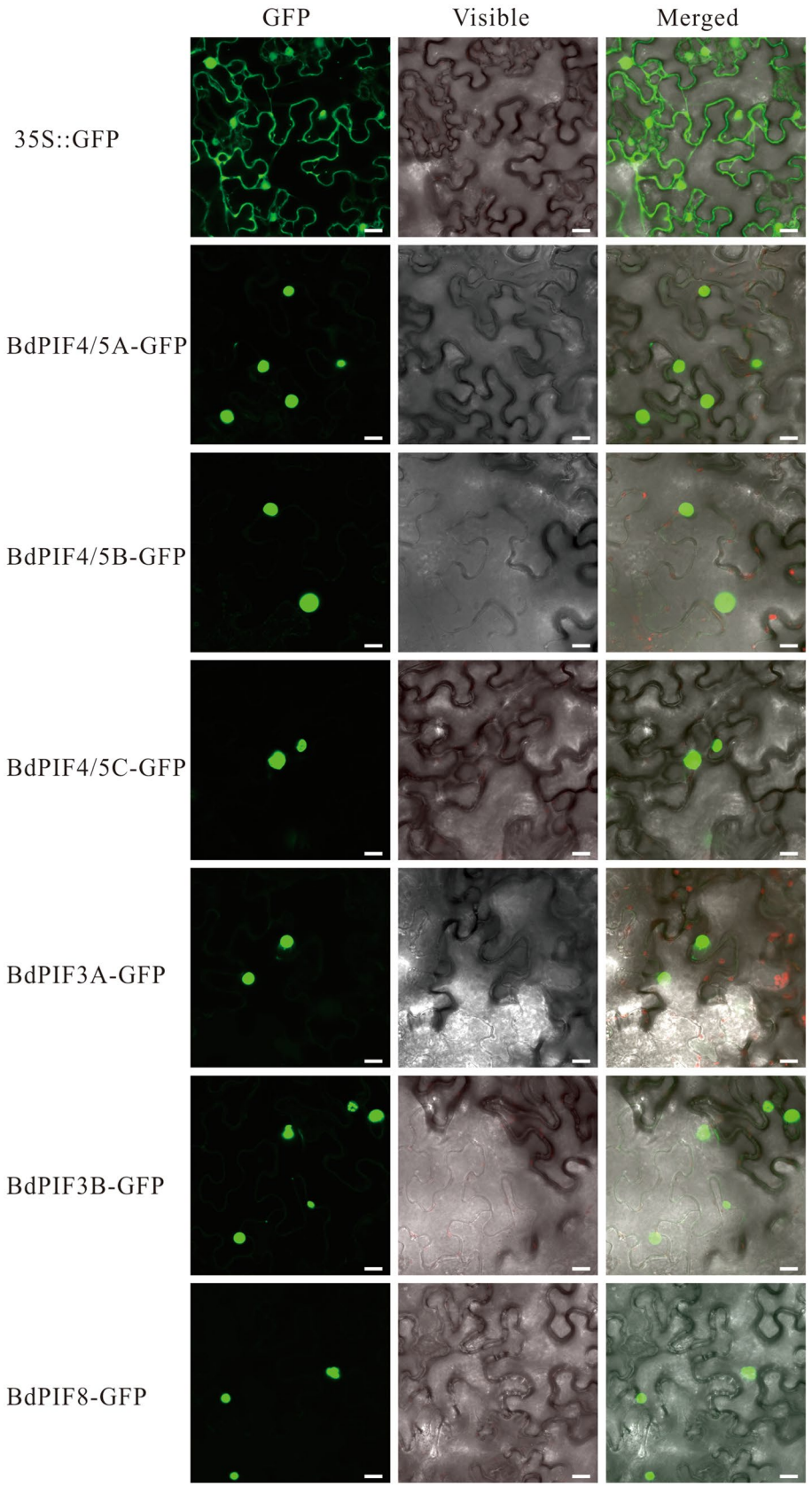

Fig. 7 Subcellular localization of BdPIFs-GFP. BdPIFs-GFP fusion proteins and GFP alone were each expressed transiently in leaves of *N. benthamiana* plants after 48 h post infiltration (hpi) and observed under a confocal laser scanning microscope in dark field for green fluorescence, white field for cell morphology and in combination, respectively. Visible, bright-field. Merged, overlay of the GFP and bright-field images. Scale bar = 100 μm

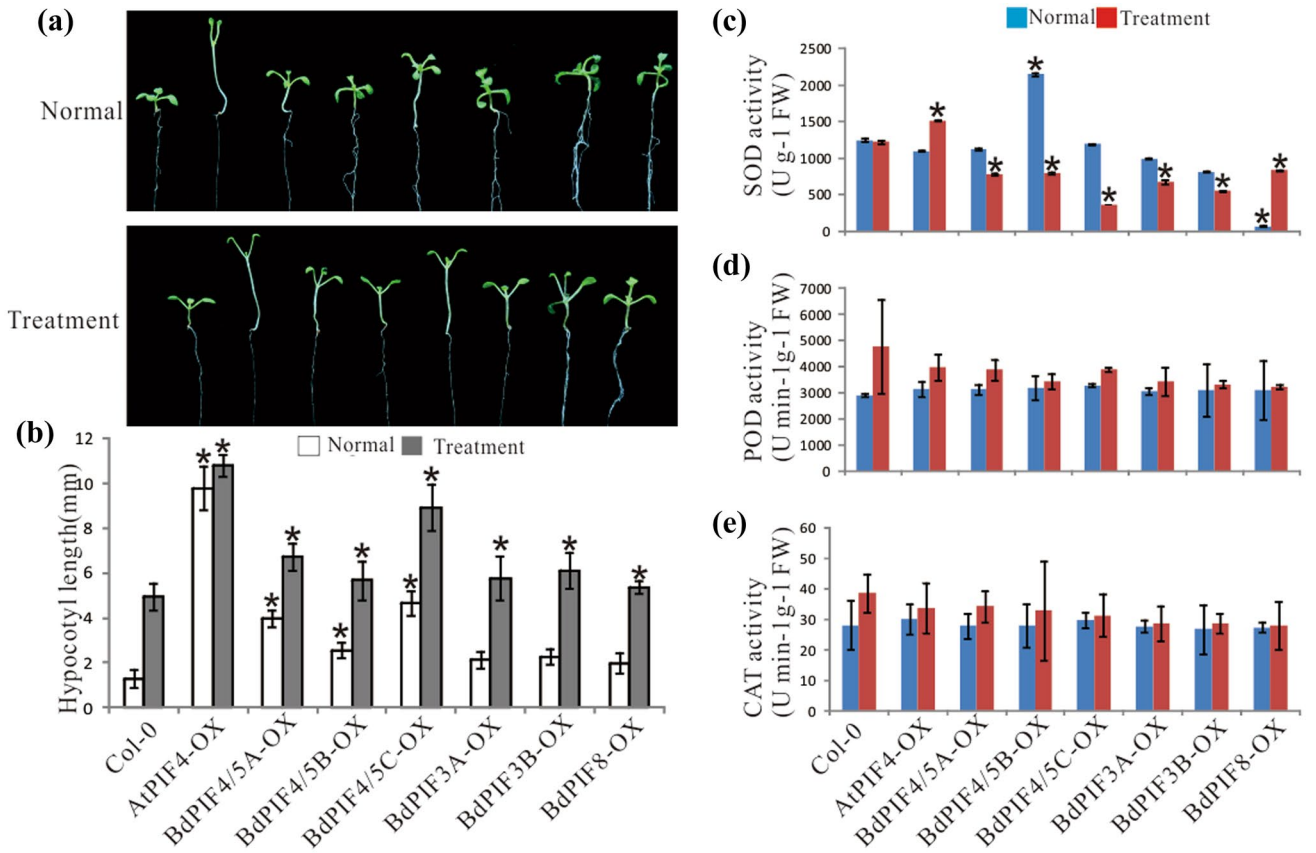

Fig. 8 Phenotypic analysis of the transgenic Arabidopsis lines expressing *BdPIF* genes under normal and light treatment conditions. Photographs **(a)** hypocotyl lengths **(b)** of Col-0, *AtPIF4-OX* and *BdPIFs-OX* seedlings grown in the 22 ℃ continuous irradiation. Plants were grown at 22 ℃ for 8 days before transfer to dark for 2 days. Control plants were maintained at light. **(c–e)**. Analysis of superoxide dismutase (SOD), peroxidase (POD) and catalase (CAT) activities. All experiments were repeated three times. Error bars indicate the standard deviation from triplicate experiments. Asterisks represent a significant difference from the light samples with Student's tests ($P \leq 0.05$)

provide new viewpoints into the origin and evolutionary history as well as function of plant PIFs.

Supplementary Information The online version contains supplementary material available at https://doi.org/10.1007/s00299-022-02850-5.

Author contributions MJ conceived and designed the work. MJ financially supported this study. MJ, CZ and GW performed the experiments and analyzed the data. MJ wrote and revised the manuscript. All authors read and approved the final manuscript.

Funding This study was supported from the Shanghai Sailing Program (19YF1414800) to MJ. The funding body had no role in study design, analysis, decision to publish, or preparation of the manuscript.

Availability of data and materials The original contributions presented in the study are included in the article/Supplementary Material; further inquiries can be directed to the corresponding author.

Declarations

Competing interests The authors declare that they have no known competing financial interests or personal relationships that could have appeared to influence the work reported in this paper.

References

Al-Sady B, Ni W, Kircher S, Schafer E, Quail PH (2006) Photoactivated phytochrome induces rapid PIF3 phosphorylation prior to proteasome-mediated degradation. Mol Cell 23:439–446. https://doi.org/10.1016/j.molcel.2006.06.011

Anderson KI, Sanderson J, Gerwig S, Peychl J (2006) A new configuration of the Zeiss LSM 510 for simultaneous optical separation of green and red fluorescent protein pairs. Cytom Part A 69A:920–929. https://doi.org/10.1002/cyto.a.20323

Arya H, Singh MB, Bhalla PL (2018) Genomic and molecular analysis of conserved and unique features of soybean PIF4. Sci Rep-UK 8:12569. https://doi.org/10.1038/s41598-018-30043-2

Bu Q, Castillon A, Chen F, Zhu L, Huq E (2011) Dimerization and blue light regulation of PIF1 interacting bHLH proteins in Arabidopsis. Plant Mol Biol 77:501–511. https://doi.org/10.1007/s11103-011-9827-4

Chen D, Xu G, Tang W, Jing Y, Ji Q, Fei Z, Lin R (2013) Antagonistic basic helix-loop-helix/bZIP transcription factors form transcriptional modules that integrate light and reactive oxygen species signaling in Arabidopsis. Plant Cell 25:1657–1673. https://doi.org/10.1105/tpc.112.104869

Choi H, Oh E (2016) PIF4 integrates multiple environmental and hormonal signals for plant growth regulation in Arabidopsis. Mol Cells 39:587–593. https://doi.org/10.14348/molcells.2016.0126

Clack T, Mathews S, Sharrock RA (1994) The phytochrome apoprotein family in Arabidopsis is encoded by five genes: the sequences and expression of PHYD and PHYE. Plant Mol Biol 25:413–427. https://doi.org/10.1007/BF00043870

Clough SJ, Bent AF (1998) Floral dip: a simplified method for *Agrobacterium*-mediated transformation of *Arabidopsis thaliana*. Plant J 16:735–743. https://doi.org/10.1046/j.1365-313x.1998.00343.x

Cordeiro AM, Figueiredo DD, Tepperman J, Borba AR, Lourenco T, Abreu IA, Ouwerkerk PB, Quail PH, Margarida Oliveira M, Saibo NJ (2016) Rice phytochrome-interacting factor protein OsPIF14 represses OsDREB1B gene expression through an extended N-box and interacts preferentially with the active form of phytochrome B. Biochim Biophys Acta 1859:393–404. https://doi.org/10.1016/j.bbagrm.2015.12.008

Fiorucci AS, Galvao VC, Ince YC, Boccaccini A, Goyal A, Allenbach Petrolati L, Trevisan M, Fankhauser C (2020) Phytochrome interacting factor 7 is important for early responses to elevated temperature in Arabidopsis seedlings. New Phytol 226:50–58. https://doi.org/10.1111/nph.16316

Goodstein DM, Shu SQ, Howson R, Neupane R, Hayes RD, Fazo J, Mitros T, Dirks W, Hellsten U, Putnam N, Rokhsar DS (2012) Phytozome: a comparative platform for green plant genomics. Nucleic Acids Res 40:D1178–D1186. https://doi.org/10.1093/nar/gkr944

Heim MA, Jakoby M, Werber M, Martin C, Weisshaar B, Bailey PC (2003) The basic helix-loop-helix transcription factor family in plants: a genome-wide study of protein structure and functional diversity. Mol Biol Evol 20:735–747. https://doi.org/10.1093/molbev/msg088

Hornitschek P, Lorrain S, Zoete V, Michielin O, Fankhauser C (2009) Inhibition of the shade avoidance response by formation of non-DNA binding bHLH heterodimers. EMBO J 28:3893–3902. https://doi.org/10.1038/emboj.2009.306

Inoue K, Nishihama R, Kataoka H, Hosaka M, Manabe R, Nomoto M, Tada Y, Ishizaki K, Kohchi T (2016) Phytochrome signaling is mediated by phytochrome interacting factor in the liverwort *Marchantia polymorpha*. Plant Cell 28:1406–1421. https://doi.org/10.1105/tpc.15.01063

International Brachypodium I (2010) Genome sequencing and analysis of the model grass *Brachypodium distachyon*. Nature 463:763–768. https://doi.org/10.1038/nature08747

Jiang M, Chu Z (2018) Comparative analysis of plant *MKK* gene family reveals novel expansion mechanism of the members and sheds new light on functional conservation. BMC Genom 19:407. https://doi.org/10.1186/s12864-018-4793-8

Jiang M, Li P, Wang W (2021) Comparative analysis of *MAPK* and *MKK* gene families reveals differential evolutionary patterns in *Brachypodium distachyon* inbred lines. PeerJ 9:e11238. https://doi.org/10.7717/peerj.11238

Jiao Y, Wickett NJ, Ayyampalayam S, Chanderbali AS, Landherr L, Ralph PE, Tomsho LP, Hu Y, Liang H, Soltis PS, Soltis DE, Clifton SW, Schlarbaum SE, Schuster SC, Ma H, Leebens-Mack J, dePamphilis CW (2011) Ancestral polyploidy in seed plants and angiosperms. Nature 473:97–100. https://doi.org/10.1038/nature09916

Jiao Y, Leebens-Mack J, Ayyampalayam S, Bowers JE, McKain MR, McNeal J, Rolf M, Ruzicka DR, Wafula E, Wickett NJ, Wu X, Zhang Y, Wang J, Zhang Y, Carpenter EJ, Deyholos MK, Kutchan TM, Chanderbali AS, Soltis PS, Stevenson DW, McCombie R, Pires JC, Wong GK-S, Soltis DE, dePamphilis CW (2012) A genome triplication associated with early diversification of the core eudicots. Genome Biol 13:R3. https://doi.org/10.1186/gb-2012-13-1-r3

Khanna R, Huq E, Kikis EA, Al-Sady B, Lanzatella C, Quail PH (2004) A novel molecular recognition motif necessary for targeting photoactivated phytochrome signaling to specific basic helix-loop-helix transcription factors. Plant Cell 16:3033–3044. https://doi.org/10.1105/tpc.104.025643

Klose C, Viczian A, Kircher S, Schafer E, Nagy F (2015) Molecular mechanisms for mediating light-dependent nucleo/cytoplasmic partitioning of phytochrome photoreceptors. New Phytol 206:965–971. https://doi.org/10.1111/nph.13207

Koini MA, Alvey L, Allen T, Tilley CA, Harberd NP, Whitelam GC, Franklin KA (2009) High temperature-mediated adaptations in plant architecture require the bHLH transcription factor PIF4. Curr Biol 19:408–413. https://doi.org/10.1016/j.cub.2009.01.046

Kumar SV, Lucyshyn D, Jaeger KE, Alos E, Alvey E, Harberd NP, Wigge PA (2012) Transcription factor PIF4 controls the thermosensory activation of flowering. Nature 484:242–245. https://doi.org/10.1038/nature10928

Kumar I, Swaminathan K, Hudson K, Hudson ME (2016) Evolutionary divergence of phytochrome protein function in *Zea mays* PIF3 signaling. J Exp Bot 67:4231–4240. https://doi.org/10.1093/jxb/erw217

Lamesch P, Berardini TZ, Li DH, Swarbreck D, Wilks C, Sasidharan R, Muller R, Dreher K, Alexander DL, Garcia-Hernandez M, Karthikeyan AS, Lee CH, Nelson WD, Ploetz L, Singh S, Wensel A, Huala E (2012) The Arabidopsis Information Resource (TAIR): improved gene annotation and new tools. Nucleic Acids Res 40:D1202–D1210. https://doi.org/10.1093/nar/gkr1090

Lau OS, Deng XW (2010) Plant hormone signaling lightens up: integrators of light and hormones. Curr Opin Plant Biol 13:571–577. https://doi.org/10.1016/j.pbi.2010.07.001

Lee N, Choi G (2017) Phytochrome-interacting factor from Arabidopsis to liverwort. Curr Opin Plant Biol 35:54–60. https://doi.org/10.1016/j.pbi.2016.11.004

Legris M, Ince YC, Fankhauser C (2019) Molecular mechanisms underlying phytochrome-controlled morphogenesis in plants. Nat Commun 10:5219. https://doi.org/10.1038/s41467-019-13045-0

Lei L, Zhou SL, Ma H, Zhang LS (2012) Expansion and diversification of the SET domain gene family following whole-genome duplications in *Populus trichocarpa*. BMC Evol Biol 12:51. https://doi.org/10.1186/1471-2148-12-51

Leivar P, Monte E (2014) PIFs: systems integrators in plant development. Plant Cell 26:56–78. https://doi.org/10.1105/tpc.113.120857

Leivar P, Quail PH (2011) PIFs: pivotal components in a cellular signaling hub. Trends Plant Sci 16:19–28. https://doi.org/10.1016/j.tplants.2010.08.003

Leivar P, Monte E, Al-Sady B, Carle C, Storer A, Alonso JM, Ecker JR, Quail PH (2008a) The Arabidopsis phytochrome-interacting factor PIF7, together with PIF3 and PIF4, regulates responses to prolonged red light by modulating phyB levels. Plant Cell 20:337–352. https://doi.org/10.1105/tpc.107.052142

Leivar P, Monte E, Oka Y, Liu T, Carle C, Castillon A, Huq E, Quail PH (2008b) Multiple phytochrome-interacting bHLH transcription factors repress premature seedling photomorphogenesis in

darkness. Curr Biol 18:1815–1823. https://doi.org/10.1016/j.cub.2008.10.058
Leivar P, Monte E, Cohn MM, Quail PH (2012) Phytochrome signaling in green Arabidopsis seedlings: impact assessment of a mutually negative phyB-PIF feedback loop. Mol Plant 5:734–749. https://doi.org/10.1093/mp/sss031
Li Q, Zhang N, Zhang L, Ma H (2015) Differential evolution of members of the *rhomboid* gene family with conservative and divergent patterns. New Phytol 206:368–380. https://doi.org/10.1111/nph.13174
Li K, Yu R, Fan LM, Wei N, Chen H, Deng XW (2016) DELLA-mediated PIF degradation contributes to coordination of light and gibberellin signalling in Arabidopsis. Nat Commun 7:11868. https://doi.org/10.1038/ncomms11868
Librado P, Rozas J (2009) DnaSP v5: a software for comprehensive analysis of DNA polymorphism data. Bioinformatics 25:1451–1452. https://doi.org/10.1093/bioinformatics/btp187
Liu Z, Zhang Y, Liu R, Hao H, Wang Z, Bi Y (2011) Phytochrome interacting factors (PIFs) are essential regulators for sucrose-induced hypocotyl elongation in Arabidopsis. J Plant Physiol 168:1771–1779. https://doi.org/10.1016/j.jplph.2011.04.009
Liu X, Chen CY, Wang KC, Luo M, Tai R, Yuan L, Zhao M, Yang S, Tian G, Cui Y, Hsieh HL, Wu K (2013) Phytochrome INTERACTING FACTOR 3 associates with the histone deacetylase HDA15 in repression of chlorophyll biosynthesis and photosynthesis in etiolated Arabidopsis seedlings. Plant Cell 25:1258–1273. https://doi.org/10.1105/tpc.113.109710
Liu S, Liu Y, Yang X, Tong C, Edwards D, Parkin IAP, Zhao M, Ma J, Yu J, Huang S, Wang X, Wang J, Lu K, Fang Z, Bancroft I, Yang T-J, Hu Q, Wang X, Yue Z, Li H, Yang L, Wu J, Zhou Q, Wang W, King GJ, Pires JC, Lu C, Wu Z, Sampath P, Wang Z, Guo H, Pan S, Yang L, Min J, Zhang D, Jin D, Li W, Belcram H, Tu J, Guan M, Qi C, Du D, Li J, Jiang L, Batley J, Sharpe AG, Park B-S, Ruperao P, Cheng F, Waminal NE, Huang Y, Dong C, Wang L, Li J, Hu Z, Zhuang M, Huang Y, Huang J, Shi J, Mei D, Liu J, Lee T-H, Wang J, Jin H, Li Z, Li X, Zhang J, Xiao L, Zhou Y, Liu Z, Liu X, Qin R, Tang X, Liu W, Wang Y, Zhang Y, Lee J, Kim HH, Denoeud F, Xu X, Liang X, Hua W, Wang X, Wang J, Chalhoub B, Paterson AH (2014) The *Brassica oleracea* genome reveals the asymmetrical evolution of polyploid genomes. Nat Commun 5:3930. https://doi.org/10.1038/ncomms4930
Liu Z, Wang Y, Fan K, Li Z, Jia Q, Lin W, Zhang Y (2021) Phytochrome-interacting factor 4 (PIF4) negatively regulates anthocyanin accumulation by inhibiting PAP1 transcription in Arabidopsis seedlings. Plant Sci 303:110788. https://doi.org/10.1016/j.plantsci.2020.110788
Luo Q, Lian HL, He SB, Li L, Jia KP, Yang HQ (2014) COP1 and phyB physically interact with PIL1 to regulate its stability and photomorphogenic development in Arabidopsis. Plant Cell 26:2441–2456. https://doi.org/10.1105/tpc.113.121657
Ma D, Li X, Guo Y, Chu J, Fang S, Yan C, Noel JP, Liu H (2016) Cryptochrome 1 interacts with PIF4 to regulate high temperature-mediated hypocotyl elongation in response to blue light. P Natl Acad Sci USA 113:224–229. https://doi.org/10.1073/pnas.1511437113
Maere S, De Bodt S, Raes J, Casneuf T, Van Montagu M, Kuiper M, Van de Peer Y (2005) Modeling gene and genome duplications in eukaryotes. P Natl Acad Sci USA 102:5454–5459. https://doi.org/10.1073/pnas.0501102102
Mittova V, Volokita M, Guy M, Tal M (2000) Activities of SOD and the ascorbate-glutathione cycle enzymes in subcellular compartments in leaves and roots of the cultivated tomato and its wild salt-tolerant relative *Lycopersicon pennellii*. Physiol Plantarum 110:42–51. https://doi.org/10.1034/j.1399-3054.2000.110106.x
Nakamura Y, Kato T, Yamashino T, Murakami M, Mizuno T (2007) Characterization of a set of phytochrome-interacting factor-Like bHLH proteins in *Oryza sativa*. Biosci Biotech Bioch 71:1183–1191. https://doi.org/10.1271/bbb.60643
Nguyen LT, Schmidt HA, von Haeseler A, Minh BQ (2015) IQ-TREE: a fast and effective stochastic algorithm for estimating maximum-likelihood phylogenies. Mol Biol Evol 32:268–274. https://doi.org/10.1093/molbev/msu300
Niu X, Chen S, Li J, Liu Y, Ji W, Li H (2019) Genome-wide identification of *GRAS* genes in *Brachypodium distachyon* and functional characterization of *BdSLR1* and *BdSLRL1*. BMC Genomics 20:635. https://doi.org/10.1186/s12864-019-5985-6
Oh E, Kim J, Park E, Kim JI, Kang C, Choi G (2004) PIL5, a phytochrome-interacting basic helix-loop-helix protein, is a key negative regulator of seed germination in *Arabidopsis thaliana*. Plant Cell 16:3045–3058. https://doi.org/10.1105/tpc.104.025163
Oh J, Park E, Song K, Bae G, Choi G (2020) Phytochrome interacting factor 8 inhibits phytochrome A-mediated far-red light responses in Arabidopsis. Plant Cell 32:186–205. https://doi.org/10.1105/tpc.19.00515
Pedmale UV, Huang SC, Zander M, Cole BJ, Hetzel J, Ljung K, Reis PAB, Sridevi P, Nito K, Nery JR, Ecker JR, Chory J (2016) Cryptochromes interact directly with PIFs to control plant growth in limiting blue light. Cell 164:233–245. https://doi.org/10.1016/j.cell.2015.12.018
Penfield S, Josse EM, Halliday KJ (2010) A role for an alternative splice variant of PIF6 in the control of Arabidopsis primary seed dormancy. Plant Mol Biol 73:89–95. https://doi.org/10.1007/s11103-009-9571-1
Prigge MJ, Otsuga D, Alonso JM, Ecker JR, Drews GN, Clark SE (2005) Class III homeodomain-leucine zipper gene family members have overlapping, antagonistic, and distinct roles in Arabidopsis development. Plant Cell 17:61–76. https://doi.org/10.1105/tpc.104.026161
Shen H, Zhu L, Castillon A, Majee M, Downie B, Huq E (2008) Light-induced phosphorylation and degradation of the negative regulator phytochrome-interacting factor 1 from Arabidopsis depend upon its direct physical interactions with photoactivated phytochromes. Plant Cell 20:1586–1602. https://doi.org/10.1105/tpc.108.060020
Shin J, Park E, Choi G (2007) PIF3 regulates anthocyanin biosynthesis in an HY5-dependent manner with both factors directly binding anthocyanin biosynthetic gene promoters in Arabidopsis. Plant J 49:981–994. https://doi.org/10.1111/j.1365-313X.2006.03021.x
Shin J, Kim K, Kang H, Zulfugarov IS, Bae G, Lee CH, Lee D, Choi G (2009) Phytochromes promote seedling light responses by inhibiting four negatively-acting phytochrome-interacting factors. P Natl Acad Sci USA 106:7660–7665. https://doi.org/10.1073/pnas.0812219106
Sun JQ, Qi LL, Li YN, Chu JF, Li CY (2012) PIF4-mediated activation of YUCCA8 expression integrates temperature into the auxin pathway in regulating Arabidopsis hypocotyl growth. Plos Genet 8:e1002594. https://doi.org/10.1371/journal.pgen.1002594
Tamura K, Stecher G, Peterson D, Filipski A, Kumar S (2013) MEGA6: Molecular evolutionary genetics analysis version 6.0. Mol Biol Evol 30:2725–2729. https://doi.org/10.1093/molbev/mst197
Tang HB, Bowers JE, Wang XY, Ming R, Alam M, Paterson AH (2008) Perspective - Synteny and collinearity in plant genomes. Science 320:486–488. https://doi.org/10.1126/science.1153917
Van Bel M, Diels T, Vancaester E, Kreft L, Botzki A, Van de Peer Y, Coppens F, Vandepoele K (2018) PLAZA 4.0: an integrative

resource for functional, evolutionary and comparative plant genomics. Nucleic Acids Res 46:D1190–D1196. https://doi.org/10.1093/nar/gkx1002

Van de Peer Y, Maere S, Meyer A (2009) The evolutionary significance of ancient genome duplications. Nat Rev Genet 10:725–732. https://doi.org/10.1038/nrg2600

Wang FF, Lian HL, Kang CY, Yang HQ (2010a) Phytochrome B is involved in mediating red light-induced stomatal opening in *Arabidopsis thaliana*. Mol Plant 3:246–259. https://doi.org/10.1093/mp/ssp097

Wang Y, Gao C, Liang Y, Wang C, Yang C, Liu G (2010b) A novel *bZIP* gene from *Tamarix hispida* mediates physiological responses to salt stress in tobacco plants. J Plant Physiol 167:222–230. https://doi.org/10.1016/j.jplph.2009.09.008

Wang X, Liu Y, Huai D, Chen Y, Jiang Y, Ding Y, Kang Y, Wang Z, Yan L, Jiang H, Lei Y, Liao B (2021) Genome-wide identification of peanut PIF family genes and their potential roles in early pod development. Gene 781:145539. https://doi.org/10.1016/j.gene.2021.145539

Whittle CA, Krochko JE (2009) Transcript profiling provides evidence of functional divergence and expression networks among ribosomal protein gene paralogs in *Brassica napus*. Plant Cell 21:2203–2219. https://doi.org/10.1105/tpc.109.068411

Wu G, Zhao Y, Shen R, Wang B, Xie Y, Ma X, Zheng Z, Wang H (2019) Characterization of maize phytochrome-interacting factors in light signaling and photomorphogenesis. Plant Physiol 181:789–803. https://doi.org/10.1104/pp.19.00239

Xu D, Deng XW (2020) CBF-phyB-PIF module links light and low temperature signaling. Trends Plant Sci 25:952–954. https://doi.org/10.1016/j.tplants.2020.06.010

Xu X, Paik I, Zhu L, Huq E (2015) Illuminating progress in phytochrome-mediated light signaling pathways. Trends Plant Sci 20:641–650. https://doi.org/10.1016/j.tplants.2015.06.010

Zhang Y, Mayba O, Pfeiffer A, Shi H, Tepperman JM, Speed TP, Quail PH (2013) A quartet of PIF bHLH factors provides a transcriptionally centered signaling hub that regulates seedling morphogenesis through differential expression-patterning of shared target genes in Arabidopsis. PLoS Genet 9:e1003244. https://doi.org/10.1371/journal.pgen.1003244

Zheng PF, Wang X, Yang YY, You CX, Zhang ZL, Hao YJ (2020) Identification of phytochrome-interacting factor family members and functional analysis of *MdPIF4* in *Malus domestica*. Int J Mol Sci 21:7390. https://doi.org/10.3390/ijms21197350